How to cite: *Angew. Chem. Int. Ed.* **2020**, *59*, 20996–21000
International Edition: doi.org/10.1002/anie.202006388
German Edition: doi.org/10.1002/ange.202006388

**Fluorescent Probes**

# An Acid-Activatable Fluorescence Probe for Imaging Osteocytic Bone Resorption Activity in Deep Bone Cavities

*Ryu Hashimoto, Masafumi Minoshima, Junichi Kikuta, Shinya Yari, Steven D. Bull, Masaru Ishii, and Kazuya Kikuchi**

***Abstract:*** *A rationally designed pH-activatable fluorescent probe (pHocas-RIS) has been used to measure localised pH levels in osteocytic lacunae in bone tissue. Conjugation of the moderate bone-binding drug risedronate to a pH-activatable BODIPY fluorophore enables the probe to penetrate osteocytic lacunae cavities that are embedded deep within the bone matrix. After injection of pHocas-RIS, any osteocytic lacunae caused by bone-resorbing osteocytes cause the probe to fluoresce in vivo, thus allowing imaging by intravital two-photon excitation microscopy. This pH responsive probe enabled the visualization of the bone mineralizing activities of acid producing osteocytes in real time, thus allowing the study of their central role in remodeling the bone-matrix in healthy and disease states.*

## Introduction

Long-lived osteocytes constitute around 90–95% of all bone cells, which exist within disk-shaped cavities called osteocytic lacunae that are present throughout the mineralized bone matrix.[1] These lacunae are interconnected by a three-dimensional canalicular network that penetrates widely throughout the bone matrix. Osteocytes project their long dendrites into these canals, which allows them to detect and modulate shear stress through communication with surface bound osteoblasts and osteoclasts that are responsible for modifying bone structures.[2] For example, osteocytes upregulate the bone resorbing activities of osteoclasts through secretion of osteoprotegerin and receptor activator of nuclear factor kappa-B ligand (RANKL), whilst they downregulate osteoblast bone forming activities through secretion of sclerostin.[3] This means that osteocytes play a central role in controlling bone remodelling pathways that are important in maintaining bone homeostasis and central to disease processes such as osteoporosis and bone cancer metastasis.[4]

Osteocytes exist deep within the bone matrix, so it is challenging to study their morphologies, activities and cellular dynamics in live animals using conventional histochemical, topographic, diffraction and imaging techniques.[5] This has led to ex vivo and in vivo imaging techniques being developed that employ fluorescence microscopy and/or fluorescent probes to image osteocytes and their associated lacuna-canalicular networks in real time. For example, transgenic reporter mice producing osteocytes that express green fluorescent proteins in their cytoplasm have been used to provide high resolution images of osteocyte dendrites oscillating within their lacunae in bone explant.[6] Alternatively, $Ca^{2+}$ binding fluorescent dyes have been used to visualize the structures of osteocytic lacuna-canalicular networks.[7]

Osteocytes are known to directly remodel the bone walls of their lacuna-canalicular systems in response to hormones produced by lactating or hibernating animals, with lacunae bone wall mineralisation producing larger cavities in a process known as osteocytic osteolysis.[8] However, the physiological role of osteocytes in direct bone mineralisation to produce $Ca^{2+}$ is still open to debate,[9] so the availability of high-resolution imaging method that would enable osteocytic osteolysis to be imaged in real time would be extremely useful. Osteocytes can directly mineralise the bone matrix of the cavity walls of their lacunae through secretion of acid from vacuolar type $H^+$-ATPases.[10] Therefore, osteocytic bone mineralisation activity can potentially be visualised indirectly through use of an OFF/ON pH sensitive fluorophore and two-photon excitation microscopic analysis to image pH levels in the lacuna-canalicular system.

The intravital imaging approach has been used to image the walls of osteocytic lacunae through application of a pH-sensitive dye (AcidiFluor™ ORANGE) to exposed surfaces of tibiae. This enabled in vivo imaging studies to be used to demonstrate that sciatic neurectomy in mice leads to a sig-

[*] R. Hashimoto, Dr. M. Minoshima, Prof. K. Kikuchi
Graduate School of Engineering, Osaka University
2-1 Yamadaoka, Suita, Osaka, 565-0871 (Japan)
E-mail: kkikuchi@mls.eng.osaka-u.ac.jp
Dr. J. Kikuta, S. Yari, Prof. M. Ishii
Department of Immunology and Cell Biology, Graduate School of Medicine and Frontier Biosciences, Osaka University
2-2 Yamadaoka, Suita, Osaka, 565-0871 (Japan)
Dr. J. Kikuta, Prof. M. Ishii, Prof. K. Kikuchi
Immunology Frontier Research Center, Osaka University
2-1 Yamadaoka, Suita, Osaka, 565-0871 (Japan)
Prof. S. D. Bull
Department of Chemistry, University of Bath
Claverton Down, Bath BA2 7AY (UK)
Prof. K. Kikuchi
Quantum Information and Quantum Biology Division, Institute for Open and Transdisciplinary Research Initiatives, Osaka University
Suita, Osaka 565-0871 (Japan)
Supporting information and the ORCID identification number(s) for the author(s) of this article can be found under: https://doi.org/10.1002/anie.202006388.

nificant increase in the pH of the osteocytic lacunae and mineralisation of the lacuna-canalicular networks in their tibiae.[7] In another ex vivo study, injection of acridine orange into mice that were pre-treated with parathyroid hormone related protein (osteocytic osteolysis promoter) enabled acidic lacunae in tibia bone explants to be imaged.[10] However, neither of these approaches are suitable for real-time visualization of local pH variations in osteocytic lacunae in live animal models, because the pH-sensitive dyes they employ are not selective for bone surfaces and so cannot produce stable well-resolved images to allow in vivo monitoring to be carried out over long periods of time.

We have previously developed reversible OFF/ON pH-sensing probes containing bisphosphonate derived alendronate fragments that bind strongly to the bone matrix that enabled visualisation of osteoclast mediated bone resorption processes.[11–13] These fluorescent probes exhibit good environmental stability, large molar absorption coefficients and high fluorescence quantum yields, which makes them well suited for visualising the low pH environments of bone surfaces in vivo. This allows their fluorescence properties at low pH to be used to monitor the bone resorption activities and motilities of osteoclasts on bone surfaces and the effect of cytokines, immune cells and drugs on their activities. For example, use of the photostable boron dipyrromethene (BODIPY) based pH-activatable fluorescent probe (pHocas-3) in transgenic reporter mice whose osteoclasts expressed tartrate-resistant acid phosphatase (TRAP)-promoter-driven red fluorescent protein (tdTomato)[14] in their mature osteoclasts enabled in vivo time-lapse imaging of osteoclast dynamics.[12] This study revealed that static osteoclasts actively promote acid mediated bone resorption, whilst motile osteoclasts do not dissolve bone surfaces. Additionally, interrogation of cellular interactions in mature osteoclasts and osteoblasts with pHocas-3 revealed that direct contact with an osteoblast resulting in an osteoclast becoming mobile and ceasing its acid secreting and bone resorption activity.[15]

Unfortunately, attempts to employ pHocas-3 for the intravital imaging of low-pH regions in osteocytic lacunae within the bones of living mice proved unsuccessful, because its strong bone binding alendronate fragments prevent it from effectively penetrating bone surfaces. Consequently, we now report herein the development of an alternative pH-activatable probe containing risedronate fragments, whose moderate bone binding affinity enables it to penetrate deep within the bone matrix. This enables this new OFF/ON pHocas-RIS probe to be used to carry out real-time intravital two-photon fluorescence imaging of acidic environments of not only bone surfaces but also osteocytic lacunae that contain acid secreting osteoclasts/osteocytes that are actively involved in bone resorption in the bones of live animals (Figure 1).

## Results and Discussion

Risedronate is a bisphosphonate drug used for the treatment of osteoporosis that binds to bone mineral through interaction with calcium ions in hydroxyapatite (HAP) in bones.[16]

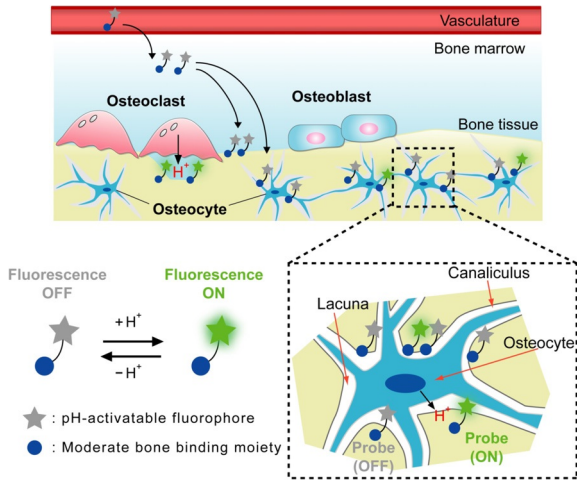


***Figure 1.*** Targeted delivery of a pH-activatable pHocas-RIS probe from the vasculature to bone surfaces and the bone walls of osteocytic lacunae. An osteocyte cell is shown in blue, the bone walls are shown in grey. The dark blue oval represents the nucleus of the osteocyte.

It exhibits lower bone binding affinity than alendronate, which enables it to distribute itself more widely throughout the bone matrix, including attachment to the walls of osteocytic lacunae.[17] Consequently, we reasoned that attachment of risedronate fragments to a pH-activatable BODIPY fluorophore would afford a new pHocas-RIS probe that could be used to visualize the low pH environments of osteocytic lacunae that contained acid secreting osteocytes (Figure 2). Two new BODIPY-containing fluorescent probes [pH-activatable pHocas-RIS and always-ON pHocas-AL-RIS (Figure 3a)] bearing bone targeting risedronate fragments were prepared through modification of a previously reported procedure involving use of a 3-aminopropane oxide linker to attach two equivalents of risedronate to a BODIPY dye (see Scheme S1 for details).[18] Reversible protonation of the basic nitrogen atom of the tertiary *para*-diethylamino group of pHocas-RIS means that it can function as an ON/OFF pH

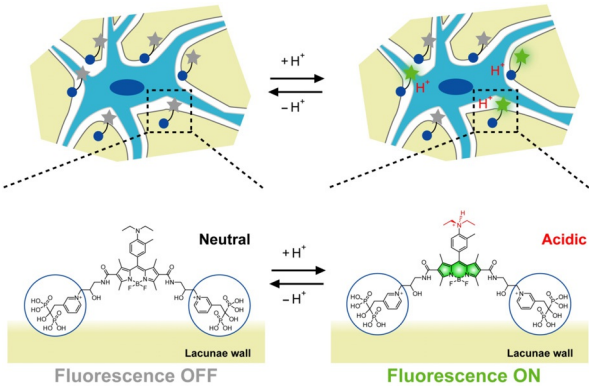


***Figure 2.*** The release of acid from osteocytes results in a decrease in the pH of their osteocytic lacunae, which results in the protonation of the diethylamino nitrogen atom of the BODIPY fluorophore. This results in PET quenching, which turns on the fluorescent activity of the BODIPY fluorophore of bone-bound pHocas-RIS.

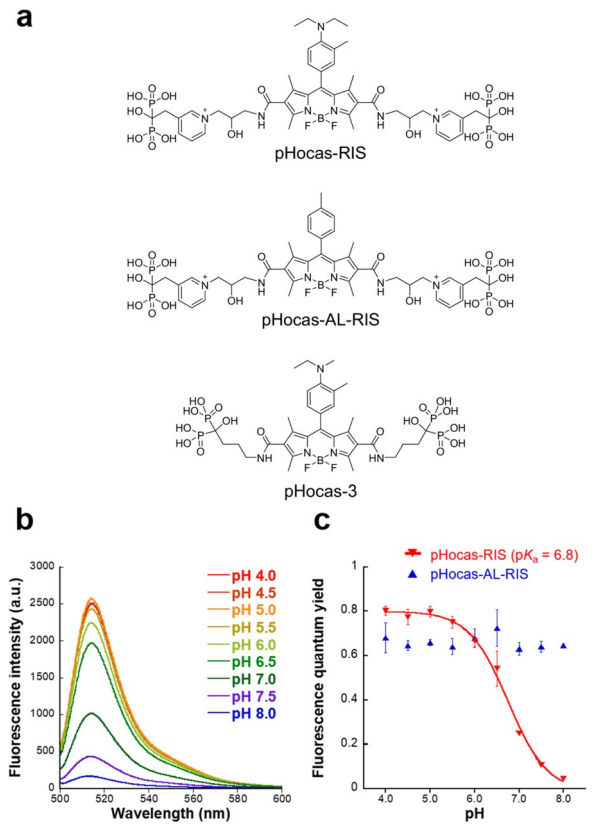


***Figure 3.*** a) Risedronate-containing pH-activatable pHocas-RIS probe, risedronate-containing always-ON pHocas-AL-RIS probe, alendronate-containing pHocas-3 probe. b) Fluorescence spectra (0.2 μM, excited at 492 nm) of pHocas-RIS in citrate-phosphate buffer (pH 4.0–8.0) with decreasing pH values. c) pH profiles of the fluorescence quantum yields of pHocas-RIS and pHocas-AL-RIS. Fluorescence quantum yields estimated using fluorescein (0.1 N NaOH, $\Phi$ 0.85) as a control. Data are presented as mean values with ± s.d. ($N = 3$).

switch to modulate the fluorescent output of the BODIPY fluorophore through a photoinduced electron transfer (PET) mechanism.[19]

The p$K_a$ value of the *N*,*N*-diethyl-2-methylaniline fragment was calculated to be around 6.6,[12] meaning that it is well suited to function as a protonatable OFF/ON switch over the pH range of 4.5–7.4 that commonly exist in lacunae.[7] pHocas-AL-RIS, which contains a BODIPY fragment with a *para*-tolyl substituent, was prepared as a control probe whose fluorescence would be "always-ON", regardless of pH.

The fluorescence quantum yields (QY) of the probes at different pH values were acquired by measuring their absorption and fluorescence emission spectra in citrate-phosphate buffer (Figure S1). The fluorescence intensity of the pHocas-RIS probe increased approximately 15-fold as the pH decreased from 8.0 to 4.0 (Figure 3b), with changes in its QY at different pH levels used to calculate the p$K_a$ value of its aniline moiety as 6.8 (Figure 3c). Conversely, as expected, the QY of pHocas-AL-RIS was found to be pH independent (Figure 3c). The QY values of protonated pHocas-RIS and pHocas-AL-RIS were similar in value to BODIPY,[12] thus indicating that the risedronate fragments had not adversely affected the probe's fluorescence properties (Table S1).

HAP samples were soaked in a solution of pHocas-RIS in buffers at different pH values (pH 4.5–8.0), with the resultant HAP bound probes then imaged using fluorescence confocal microscopy. The fluorescence signals of the HAP particles treated with pHocas-RIS were very weak at pH 8.0 (Figure S2a), with the fluorescence intensity of the HAP-probe samples increasing dramatically at low-pH (pH 5.0), which was similar to the pH fluorescence response of the free probe in aqueous solution.

Conversely, as expected, the fluorescence intensity of HAP particles bound to always-ON pHocas-AL-RIS probe remained constant over the pH range from 4.5–8.0 (Figure S2b). No dissociation of either risedronate-conjugated probes from the HAP particles were observed over time, thus indicating that both probes remained permanently bound to HAP over the time-course of these imaging experiments. These probes exhibit no cytotoxicity against cultured RAW264.7 cells that can be differentiated into osteoclasts (Figure S3), whilst pHocas-RIS did not inhibit RANKL-induced osteoclastogenesis (Figure S4).

Imaging studies were then carried out using transgenic TRAP-tdTomato mice containing osteoclasts expressing a red fluorescent protein.[14] Daily subcutaneous administration of both probes (5 mg kg$^{-1}$) to these genetically modified mice over a 3 day period was followed by their anaesthetisation and two-photon imaging of the medullary cavities of their thin calvaria parietal bones. Processing of the images were carried out using spectroscopic unmixing algorithms that enabled fluorescence signals from the probe (green), tdTomato (red) and second-harmonic generation (SHG) emissions of bone collagen fibres (blue) to be distinguished. Green fluorescence signals from pHocas-AL-RIS were present across the entire parietal bone surface (Figure 4, top left), thus indicating that the risedronate-conjugated probe was evenly distributed over the bone surface. pHocas-AL-RIS and pHocas-AL could be detected at bone surfaces around 2–3 min after bolus injection (Figures S5, S6, Movies S1, and S2), thus indicating that this class of probe is rapidly adsorbed from blood plasma to bone tissue (Figure S5).

The fluorescent output of pHocas-AL-RIS on external bone surfaces were not decreased after 90 min (Figure S7 and Movie S3), thus demonstrating that the BODIPY fluorophore is sufficiently photostable to be used for real time in vivo imaging of bone surfaces over extended periods of time. Imaging studies (from a lateral view) revealed the presence of green fluorescence signals from protonated pH-activatable pHocas-RIS produced from the action of stationary acid secreting osteoclasts in direct contact with bone surfaces within the bone marrow cavity (Figure 4, middle). Images of bone surfaces (viewed from above) showed local overlap of protonated pHocas-RIS signals (green) that were coincident with osteoclasts expressing the TRAP-tdTomato gene (red) (Figure 4, bottom). Time-lapse imaging could be used to explore spatiotemporal changes in bone acidification levels induced by the action of osteoclasts (Figure S8 and Movie S4), with the fluorescence output of protonated pHocas-RIS enabling the appearance of acidified bone surfaces to be detected in real time. As demonstrated in our previous studies,[11,12] overlap of the green fluorescence signals of the

  

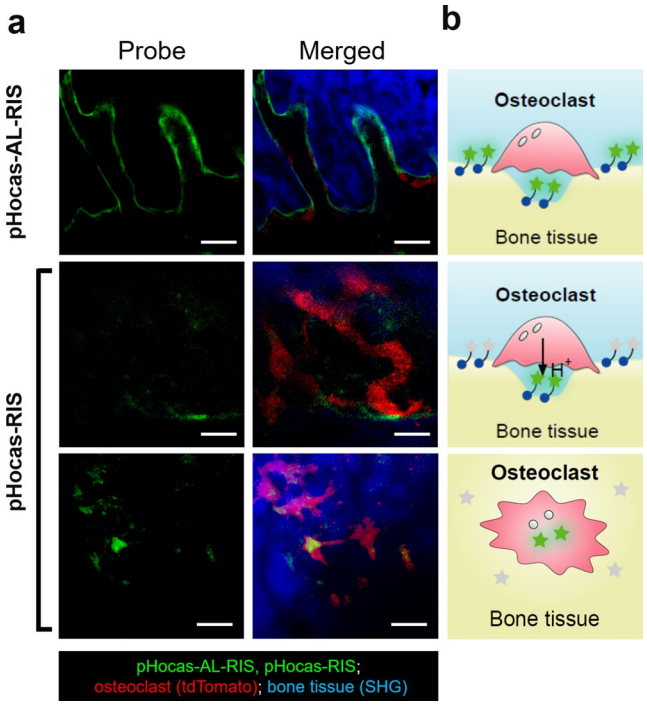


***Figure 4.*** a) Two-photon excitation imaging of pHocas-AL-RIS and pHocas-RIS in the bone tissue of living transgenic mice. Emissions: pHocas probes in green, tdTomato protein in osteoclasts in red, collagen in bone matrix in blue. Excitation wavelength = 940 nm. Scale bars = 50 μm (pHocas-AL-RIS, top), 20 μm (pHocas-RIS, middle), and 50 μm (pHocas-RIS, bottom). Second harmonic generation from collagen in the bone matrix is responsible for blue fluorescent signals. b) Schematic illustration of bone tissues.

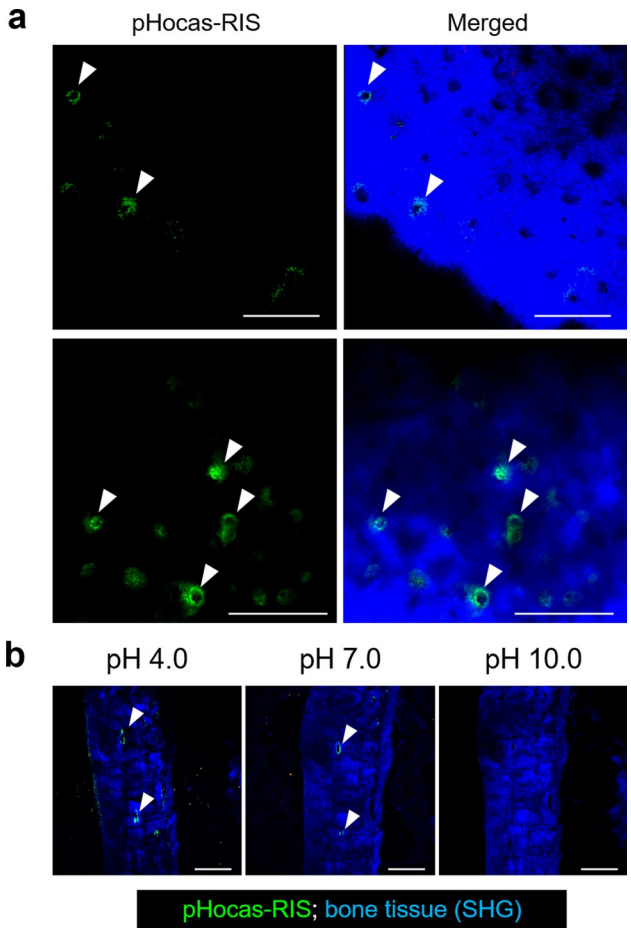


***Figure 5.*** a) Two-photon excitation imaging reveals green fluorescent regions (see white arrows) corresponding to protonated pHocas-RIS bound to the walls of acidic osteocytic lacunae in calvaria parietal bones. Dose: 5 mg kg$^{-1}$ (top), 10 mg kg$^{-1}$ (bottom) for 3 days. Excitation wavelength = 940 nm. Scale bar = 100 μm. b) Two-photon excitation imaging of bone tissue cryosections at different pH (pH 4.0, pH 7.0, pH 10.0). Bone cryosections obtained from mice pre-treated with pHocas-RIS that were then pre-soaked in buffers of different pH prior to imaging. Scale bar = 150 μm. White arrows indicate green fluorescent regions corresponding to protonated pHocas-RIS bound to the walls of acidic osteocytic lacunae. Second harmonic generation from collagen in the bone matrix is responsible for blue background signals.

new pH-activatable pHocas-RIS probe with the red fluorescent signals of osteoclasts enabled active acid secreting osteoclasts (bone-resorptive) to be readily discriminated from inactive (non bone-resorptive) osteoclasts.

Further imaging studies revealed the presence of small numbers of ring-shaped green fluorescence signals of the protonated pHocas-RIS that were present in bone obtained from deep cortical regions. It is proposed that these fluorescent signals originate from probes bound to the walls of osteocytic lacunae that contained bone resorptive osteocytes that were actively secreting acid to create a low pH environment (Figure 5a). The relatively low numbers of these fluorescence signals reflect the fact that only a small number of osteocytes are thought to be actively resorbing bone matrix under normal physiological conditions. As expected, our previously reported pHocas-3 probe containing the high bone-affinity alendronate fragment was incapable of penetrating bone surfaces to image osteocytic lacunae (Figure S9). The pH responsiveness of the pHocas-RIS probe within the lacunae of the bone matrix was confirmed by carrying out ex vivo fluorescent imaging of cryogenically prepared deep bone slices at different pH levels (Figure 5b and Figure S10). These studies revealed the presence of strong fluorescent signals for osteocytic lacunae in a bone section treated at pH 4.0, reduction in fluorescent intensity of a bone section at pH 7.0, and no fluorescence for a bone section treated at pH 10.0. This clearly demonstrated that the intensity of the pH-activatable fluorescent response of the pHocas-RIS probe can be used to effectively image the pH of osteocytic lacunae in living bone. This should enable the probe to be used to visualize the pharmacokinetics of osteoclast and osteocyte mediated bone remodeling processes and help delineate the role that osteocytes play in controlling bone homeostasis in health, aging and disease.

## Conclusion

A new fluorescent pHocas-RIS probe containing a risedronate fragment with moderate bone-binding affinity has been used to visualize the pH environments of osteocytic lacunae in bone tissue. Intravital two-photon fluorescent

  

imaging studies using this probe revealed the presence of acidic regions on bone surfaces produced through the action of acid secreting osteoclasts that are responsible for dissolving bone mineral. This new probe was shown to be able to penetrate deep within bone tissues, which enabled it to be used for in vivo imaging of osteocytic lacunae containing bone resorbing osteocytes that produce acidic microenvironments. We anticipate that use of these probes in tandem with transgenic mice that express fluorescently labeled bone cells will enable real time imaging of osteocyte mediated bone resorptive processes that are important in remodeling bone-matrix in aging, health and disease.

## Acknowledgements

This research was supported by the following grants: Grants-in-Aid for Scientific Research (16K01933, 20K05747 to M. Minoshima, 19K17906 to J. Kikuta, 19H056570 to M. Ishii, 18H03935, 19K22255 to K. Kikuchi); Innovative Areas "Frontier Research on Chemical Communications" of Ministry of Education (17H06409); Culture, Sports, Science, and Technology (MEXT) of Japan; CREST, Japan Science and Technology (JST) Agency (JPMJCR15G1 to M. Ishii); PRIME (JP19gm6210005 to J. Kikuta); Japan Agency for Medical Research and Development (AMED) (18he0902005h0004, 17ae0101041h9902, 18fm0208018h0002 to K. Kikuchi); Takeda Science Foundation; JSPS A3 Foresight Program; and JSPS CORE-to-CORE Program "Asian Chemical Biology Initiative"; Japan (JSPS)-UK (RSC) Research Cooperative Program (JPJSBP120195705 to K. Kikuchi); Royal Society International Exchange (IEC\R3\183068 to S. D. Bull).

## Conflict of interest

The authors declare no conflict of interest.

**Keywords:** fluorescent probes · intravital imaging · osteocytes · osteocytic lacunae · pH-activatable probes

[1] A. G. Robling, L. F. Bonewald, *Ann. Rev. Physiol.* **2020**, *82*, 485 – 506.
[2] A. Vatsa, R. G. Breuls, C. M. Semeins, P. L. Salmon, T. H. Smit, J. Klein-Nulend, *Bone* **2008**, *43*, 452 – 458.
[3] G. Y. Rochefort, S. Pallu, C. L. Benhamou, *Title Osteoporosis Int.* **2010**, *21*, 1457 – 1469.
[4] J. T. Compton, F. Y. Lee, *J. Bone Joint. Surg.* **2014**, *96A*, 1659 – 1668.
[5] K. D. Harrison, D. M. L. Cooper, *Front. Endocrinol.* **2015**, *6*, 122.
[6] S. L. Dallas, P. A. Veno, *Methods Mol. Biol.* **2012**, *816*, 425 – 457.
[7] H. Sano, J. Kikuta, M. Furuya, N. Kondo, N. Endo, M. Ishii, *Bone* **2015**, *74*, 134 – 139.
[8] E. Tsourdi, K. Jaehn, M. Rauner, B. Busse, L. F. Bonewald, *J. Musc. Neuron. Int.* **2018**, *18*, 292 – 303.
[9] N. K. Wittig, M. E. Birkbak, F. L. Bach-Gansmo, A. Pacureanu, M. H. Wendelboe, A. Bruel, J. S. Thomsen, H. Birkedal, *Calcif. Tissue Int.* **2019**, *105*, 308 – 315.
[10] K. Jähn, S. Kelkar, H. Zhao, Y. Xie, L. M. Tiede-Lewis, V. Dusevich, S. L. Dallas, L. F. Bonewald, *J. Bone Miner. Res.* **2017**, *32*, 1761 – 1772.
[11] T. Kowada, J. Kikuta, A. Kubo, M. Ishii, H. Maeda, S. Mizukami, K. Kikuchi, *J. Am. Chem. Soc.* **2011**, *133*, 17772 – 17776.
[12] H. Maeda, T. Kowada, J. Kikuta, M. Furuya, M. Shirazaki, S. Mizukami, M. Ishii, K. Kikuchi, *Nat. Chem. Biol.* **2016**, *12*, 579 – 585.
[13] M. Minoshima, J. Kikuta, Y. Omori, S. Seno, R. Suehara, H. Maeda, H. Matsuda, M. Ishii, K. Kikuchi, *ACS Cent. Sci.* **2019**, *5*, 1059 – 1066.
[14] J. Kikuta, Y. Wada, T. Kowada, Z. Wang, G. H. Sun-Wada, I. Nishiyama, et al., *J. Clin. Invest.* **2013**, *123*, 866 – 873.
[15] M. Furuya, J. Kikuta, S. Fujimori, S. Seno, H. Maeda, M. Shirazaki, M. Uenaka, H. Mizuno, Y. Iwamoto, A. Morimoto, K. Hashimoto, T. Ito, Y. Isogai, M. Kashii, T. Kaito, S. Ohba, U. Chung, A. C. Lichtler, K. Kikuchi, H. Matsuda, H. Yoshikawa, M. Ishii, *Nat. Commun.* **2018**, *9*, 300.
[16] R. G. G. Russell, M. J. Rogers, *Bone* **1999**, *25*, 97 – 106.
[17] A. J. Roelofs, F. P. Coxon, F. H. Ebetino, M. W. Lundy, Z. J. Henneman, G. H. Nancollas, S. Sun, K. M. Blazewska, J. L. Bala, B. A. Kashemirov, A. B. Khalid, C. E. McKenna, M. J. Rogers, *J. Bone Miner. Res.* **2010**, *25*, 606 – 616.
[18] S. Sun, K. M. Błażewska, A. P. Kadina, B. A. Kashemirov, X. Duan, J. T. Triffitt, J. E. Dunford, R. G. G. Russell, F. H. Ebetino, A. J. Roelofs, F. P. Coxon, M. W. Lundy, C. E. McKenna, *Bioconjugate Chem.* **2016**, *27*, 329 – 340.
[19] Y. Urano, D. Asanuma, Y. Hama, Y. Koyama, T. Barrett, M. Kamiya, T. Nagano, T. Watanabe, A. Hasegawa, P. L. Choyke, H. Kobayashi, *Nat. Med.* **2009**, *15*, 104 – 109.

Manuscript received: May 2, 2020
Revised manuscript received: June 24, 2020
Accepted manuscript online: August 3, 2020
Version of record online: September 8, 2020

  